PHYSICAL REVIEW E VOLUME 48, NUMBER 6 DECEMBER 1993

Two-dimensional Landau–de Gennes dynamical model for the unwinding transition of a cholesteric liquid crystal

T. Frisch, L. Gil, and J. M. Gilli
Institut de Nonlinéaire de Nice, Université de Nice Sophia Antipolis, Parc Valrose, F-06034 Nice Cedex, France
(Received 30 September 1993)

In this Rapid Communication we derive a simple dynamical model for the unwinding transition of a cholesteric liquid crystal. Our model describes not only the equilibrium but also the nonequilibrium features of the transition. In particular, our model is in qualitative agreement with the experimental observations of systems containing rotating spiral waves, all of the same handedness.

PACS number(s): 64.70.Md, 47.20.Ky, 05.45.+b

The spontaneous creation of spiral waves has been commonly observed in nonequilibrium systems in fields, such as biology [1], chemistry [2], hydrodynamics [3], and nonlinear optics [4]. In all such systems, spiral waves appear in pairs with opposite topological charge and opposite handedness (sense of rotation). Now, beside those results, recent experimental observations [5] dealing with the unwinding transition of a cholesteric liquid crystal [6–9] report the spontaneous nucleation of rotating spiral waves with only one handedness. To our knowledge, those time-dependent structures have not yet been investigated theoretically. The aim of this Rapid Communication is then to derive a simple dynamical bidimensional model for the unwinding transition of a cholesteric liquid crystal which explains the uniqueness of the spiral handedness.

In the unwinding transition problem, a large-pitch cholesteric liquid crystal is sandwiched between two horizontal parallel glass plates, with homeotropic anchoring (i.e., the molecules near the surface are perpendicular to the plates). When the distance d between the two plates is small enough, the boundary conditions force all the molecules throughout the sample to be perpendicular to the plates. On the contrary, above a critical distance d_c, cholesteric winding takes place. In such a system, an ac electric field is usually applied perpendicularly to the horizontal glass plates, in order to modify the molecular orientation through the dielectric anisotropy of the liquid crystal. According to the literature of the subject, two distinct kinds of dynamical behavior have been observed, depending on the frequency of the applied electric field. When a high-frequency electric field is used to avoid charge injection, the system is described by a Lyapunov function (the dynamics is ruled by a minimization principle). In that case, the thermodynamical phase diagram displays a homeotropic nematic phase, isolated fingers, fingerprint patterns [6], spherulitic bubble domains [7,8], translationally invariant cholesteric configuration (TIC), and a modulated TIC phase [9]. In contrast, when a dc electric field is applied, the system is out of equilibrium and displays steady time-dependent structures. In that case the literature reports the formation of Archimedian spirals [5], rotating around their core with a single given handedness.

Let us now develop a two-dimensional (2D) model of the unwinding cholesteric transition, able to describe both the various equilibrium and out-of-equilibrium liquid-crystal textures. However, we are not interested in a microscopic exact description of the complex dynamical physical mechanism involved [10], but rather in a Landau–de Gennes approach, which only takes into account the symmetries of the problem.

We introduce the following convenient notations:

$$Q=n_z(n_x+in_y),\quad \partial\chi=\partial x+i\partial y\ ,$$

and

$$\bar{Q}=n_z(n_x-in_y),\quad \partial\bar{\chi}=\partial x-i\partial y\ ,$$

in which n_x, n_y, and n_z are the components of the director $\mathbf{n}$. With our definitions, the plates are perpendicular to the z axis and the homeotropic state corresponds to $n_x=n_y=0$ and $n_z=1$. Close to the nematic-cholesteric transition the director is well described by

$$\mathbf{n}\simeq\begin{pmatrix}\cos\left[\frac{z}{p}+\theta\right]\sin\left[\alpha\sin\left[\frac{\pi z}{d}\right]\right]\\ \sin\left[\frac{z}{p}+\theta\right]\sin\left[\alpha\sin\left[\frac{\pi z}{d}\right]\right]\\ \cos\left[\alpha\sin\left[\frac{\pi z}{d}\right]\right]\end{pmatrix},$$

where p is the cholesteric pitch, α is the maximum azimuth deviation from the homeotropic situation, and where α and θ slowly depend on x, y, and t [11]. As shown in Refs. [11,12], there exists a range of parameters for which the transition is second order or weakly first order. In such a parameter region, α is small and the director may be expressed as

$$Q=\sin\left[\frac{\pi z}{d}\right]e^{iqz}A(x,y,t)+O(A^2)$$

$$\text{with}\quad A(x,y,t)=\alpha e^{i\theta}\ ,$$

where A is the order parameter of the transition, invari-

ant by the transformation $\mathbf{n}\rightarrow-\mathbf{n}$. For the thermodynamic transition, the equation we look for must be associated with a Lyapunov function $\mathcal{F}$ [13] and therefore can be expressed as

$$\frac{\partial A}{\partial t}=-\frac{\delta\mathcal{F}}{\delta\overline{A}}\ , \tag{1}$$

where $\mathcal{F}$ is real and generalizes the two-dimensional liquid-crystal free-energy density. Now, close to the transition, the order parameter A and its spatial derivatives are small and, consequently, we can search for an expression of $\mathcal{F}$ as a Taylor expansion in $A,\partial_\chi A,\partial_{\chi\chi}A,\ldots$. At each order in A, we will limit ourselves to spatial derivatives up to second order, as this is already the case in Frank's expression of the free-energy density [14]. The invariance of the system with respect to rotation around the z axis and the rotation of 180° around the x axis are, respectively, expressed as

$$\mathcal{F}\rightarrow\mathcal{F},\quad \partial_\chi\rightarrow e^{i\theta}\partial_\chi,\quad A\rightarrow e^{i\theta}A\ ,$$

and

$$\mathcal{F}\rightarrow\mathcal{F},\quad \partial_\chi\rightarrow\partial_{\overline{\chi}},\quad A\rightarrow\overline{A}\ .$$

Combinations of those two symmetries, together with the fact that $\mathcal{F}$ is real, restrict the possible second-order terms to

$$\mathcal{F}_2=\mathcal{F}_2(|A|^2,|A_\chi|^2,|A_{\overline{\chi}}|^2,(A_{\overline{\chi}}^2+\overline{A}_\chi^2),(A_{\chi\overline{\chi}}\overline{A}+\overline{A}_{\chi\overline{\chi}}A),(A_{\overline{\chi}\overline{\chi}}A+\overline{A}_{\chi\chi}\overline{A}))\ ,$$

where A_χ ($A_{\overline{\chi}}$) stands for the partial derivative of A with respect to χ ($\overline{\chi}$). Performing the same kind of analysis to third order leads to

$$\mathcal{F}_3=\mathcal{F}_3(A^2\overline{A}_{\overline{\chi}}+\overline{A}^2A_\chi,|A|^2(A_{\overline{\chi}}+\overline{A}_\chi))$$

and to the nine following terms:

$$\mathcal{F}_4=\mathcal{F}_4=\begin{bmatrix} |A|^4,|A|^2|\overline{A}_\chi|^2,|A|^2|A_\chi|^2,|A|^2(A_{\overline{\chi}}^2+\overline{A}_\chi^2), \\ |A|^2(AA_{\overline{\chi}\overline{\chi}}+\overline{A}\,\overline{A}_{\chi\chi}),|A|^2(A\overline{A}_{\chi\overline{\chi}}+\overline{A}A_{\chi\overline{\chi}}), \\ A^3\overline{A}_{\overline{\chi}\overline{\chi}}+\overline{A}^3A_{\chi\chi},A^2A_{\overline{\chi}}\overline{A}_{\overline{\chi}}+\overline{A}^2\overline{A}_\chi A_\chi,A^2\overline{A}_\chi\overline{A}_{\overline{\chi}}+\overline{A}^2A_{\overline{\chi}}A_\chi \end{bmatrix}$$

for order 4. In $\mathcal{F}_4$, one could be tempted to neglect the eight terms involving spatial derivatives, which are *a priori* slowly varying in space, and to retain only $|A|^4$ in the free energy. Unfortunately it is easy to prove analytically and numerically that the corresponding free-energy density does not have a lower bound, and that at least one of the nonhomogeneous fourth-order terms is needed for the boundedness. There is no deep reason to select one of the terms rather than another. However, for the sake of simplicity, we will limit ourselves, in what follows, to the three terms $|A|^4,|A|^2|\overline{A}_\chi|^2,|A|^2|A_\chi|^2$. Then the dynamics associated with Eq. (1) reads, after some simple scaling transformations on space, time, and the modulus of A,

$$\frac{\partial A}{\partial t}=\mu A+A_{\chi\overline{\chi}}-\delta\overline{A}_{\chi\chi}+\eta(AA_{\overline{\chi}}-\overline{A}A_\chi)-|A|^2A$$
$$+\zeta(|A|^2A_{\chi\overline{\chi}}+\overline{A}A_\chi A_{\overline{\chi}})\ . \tag{2}$$

In this equation, μ is the growth rate of the instability and is roughly proportional to $d-d_c$, δ is related to the anisotropy of the liquid crystal (relative differences between the elastic constants [14], η is proportional to the chirality, and finally ζ is needed for the boundedness of the free energy. This equation is of the Ginzburg-Landau type. However, it admits two new terms. The first one is $\overline{A}_{\chi\chi}$ and, as shown in Ref. [15], it conveys the anisotropy of the liquid crystal. The second term, $AA_{\overline{\chi}}-\overline{A}A_\chi$, which is not invariant by the mirror symmetry $(x,y,z)\rightarrow(x,-y,z)$, expresses the intrinsic chirality of the cholesteric.

In order to compare our model with the rigorous phase diagram of Ref. [16], we now perform a simple analysis of Eq. (2). $A_0=0$ is a trivial solution of Eq. (2), corresponding to the homeotropic phase. It is linearly stable for negative values of μ. For positive values of μ, there exists a nonzero homogeneous solution, $A_H=i\sqrt{\mu}$, corresponding to the TIC solution with $\theta=\pi/2$ [10] whose critical eigenvalue is given by

$$\sigma(\mathbf{k})=-(1-\delta+\mu\zeta-2\eta^2)k_x^2-(1+\delta+\mu\zeta)k_y^2+O(k^4)\ ,$$

where $\mathbf{k}=(k_x,k_y)$ is the Fourier wave vector. Therefore, for $\eta^2>(1-\delta+\mu\zeta)/2$, the TIC is unstable with respect to spatial perturbations. The critical wave vector corresponding to the highest instability rate is then proportional to the chiral coefficient η. Using a fourth-order Runge-Kutta scheme, with spatial derivatives computed with either finite-difference algorithms or Fourier transforms, we have numerically checked that, in such a case, this bifurcation gives rise to a periodic pattern, identifiable with the classical modulated TIC. Furthermore, in the parameter range where the homeotropic state is stable ($\mu<0$), we numerically observed isolated subcritical localized structures, which can be identified as the cholesteric finger structures. These fingers are obtained for quite high values of the chiral coefficient η and look like those reported by the previous experimental and analytical works [Fig. 1(a)]. Especially, the two ends of the finger are not identical, one (the abnormal tip) being sharper than the other (the normal one). Furthermore,

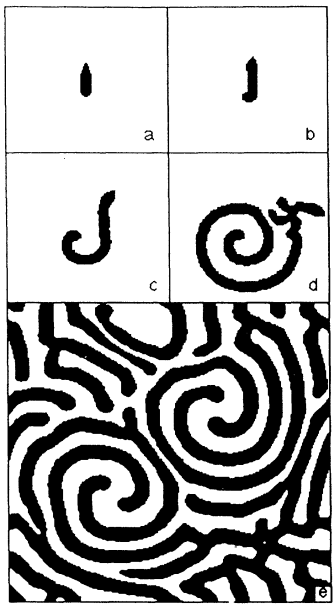

FIG. 1. Numerical simulation of Eq. (3) showing $|A|$ vs x and y. The contrast has been enhanced, the white corresponding to $|A|=0$ and the black to the nonvanishing value of the modulus. We have used periodic boundary conditions, and the size of the square box is 102.4. Initial values have been chosen to fit at best the isolated finger structure. $\mu=-0.25$, $\delta=-0.3$, $\eta=2.7$, $\zeta=1$, and $\nu_1=\nu_2=0$. (a) displays the equilibrium finger solution ($\nu_0=0$) after some time evolution. The finger length is twice the initial one. (b), (c), and (d) are successive pictures of the temporal evolution obtained with $\nu_0=0.1$. For (e), which corresponds to the long-time behavior, random initial values have been used.

fingers with two normal rounded tips but with a $+1$ disclination in their bulk are also observed [8]. The connection topological rules, with a repulsion between normal ends, the collapse of two ends of opposite sign, and the T-like sidebranching [16] have been numerically observed. From a qualitative point of view, these observations are related to the presence of the chiral term η $(AA_{\bar{\chi}}-\bar{A}A_{\chi})$ and not to the fourth-order terms which have been chosen in order to saturate the instability. These numerical and analytical results as a whole are summarized in Fig. 2. Remarkably, the phase diagram does display two triple points, as in the experimental and theoretical thermodynamic phase diagrams obtained in Ref. [16]. We believe that if the omitted fourth-order terms were taken into consideration, the phase diagram in the neighborhood of $\mu=0$ would only be modified in a quantitative way, but not in a qualitative one. Now we tackle the nonequilibrium dynamics and the formation of horizontal birefringent spiral structures in the cholesteric liquid crystal, induced by a dc or ac vertical electric field. In contrast to the microscopic interpretation of Hinov and Kukleva [5], for which the spiral patterns could be explained by possible gradient flexoelectric generation of point singularities, we adopt here a different point of view. Indeed, a small vertical electric field can be modeled by supplementary terms in the dynamical equation (2). These new terms can be derived using the previ-

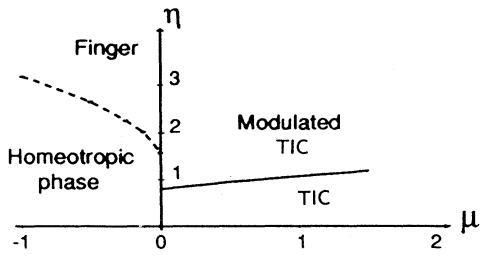

FIG. 2. Thermodynamical phase diagram of Eq. (2) vs (μ,η). We have used $\delta=-0.3$ and $\zeta=1$. The dashed line is a numerical result.

ous symmetry arguments, except that the turnover symmetry transformation is now modified in the following way:

$$\mathcal{T}\rightarrow\mathcal{T},\quad \partial_{\chi}\rightarrow\partial_{\bar{\chi}},\quad A\rightarrow\bar{A},\quad E_z\rightarrow -E_z\ .$$

The change of sign of E_z in the previous expression is fundamental. It leads, at first order in A to a complexification of the real coefficients, and induces a dynamics that cannot be described by a Lyapunov function. The resulting pertubated equation is then

$$\begin{aligned}\frac{\partial A}{\partial t}=&[\mu+i\nu_0E_z\cos(\omega t)]A+[1+i\nu_1E_z\cos(\omega t)]A_{\chi\bar{\chi}}\\&-[\delta+i\nu_2E_z\cos(\omega t)]\bar{A}_{\chi\chi}+\eta(AA_{\bar{\chi}}-\bar{A}A_{\chi})\\&-|A|^2A+\zeta(|A|^2A_{\chi\bar{\chi}}+\bar{A}A_{\chi}A_{\bar{\chi}})\ ,\end{aligned}\tag{3}$$

where ν_0,ν_1,ν_2 are real coefficients and ω is the electric-field frequency. Note that corrections to the real coefficients will be neglected here since they are at least of second order in E_z. Also we will not take into account the corrections to the nonlinear terms because of the smallness of A.

Numerical simulations of Eq. (3) with $\omega=0$ and arbitrary initial conditions reveal the formation of Archimedian spiral waves with a single given handedness [Fig. 1(e)]. The sense of rotation can be easily reversed by either changing the sign of the chirality (η) or the sign of the electric field (νE). As in our preliminary experimental results [17] or in Ref. [5], we observed that each spiral consists of the rolling up of a drifting finger (Fig. 3).

The formation of one spiral can be numerically investigated in the following way. Starting from an isolated finger, and increasing ν_0 up to a weak nonvanishing value, we observe a drift of the central part of the finger perpendicularly to its local axis. As in excitable media [2], the velocity of the drift is nonuniform all along the finger [Fig. 1(b)]. The velocity being the slowest at the rounded end, the finger rolls up of around its normal tip and forms a spiral [Figs. 1(c) and 1(d)]. In contrast, the abnormal end, which is the fastest part of the finger, seems to be the center of a sidebranching mechanism.

We have numerically checked that this perpendicular displacement of the finger is due to the ν_i coefficients, and its direction is imposed by the sign of the chiral coefficient. This mechanism is robust and is found to persist in one space dimension. Indeed, in the parameter region where the isolated fingers are stable, we do numeri-

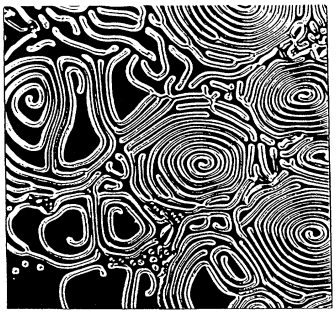

FIG. 3. Experimental observation at the ambient temperature of an MBBA-CB15 mixture with a small amount of chiral material ($\Delta\epsilon>0$). The sample is a few micrometers thick and the picture is one millimeter wide. A 1.5-dc voltage is applied between the slides.

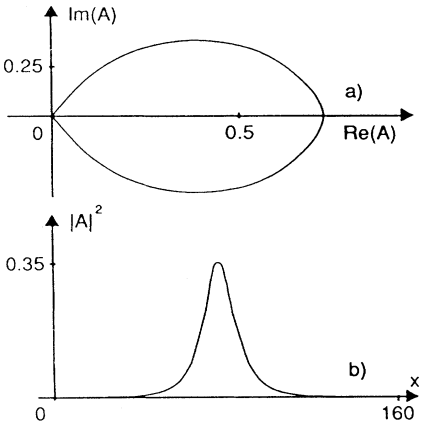

FIG. 4. Numerical simulation of the restriction of Eq. (3) to one space dimension. $\mu=-0.1$, $\eta=2.0$, $\zeta=1$, and $\nu_0=\nu_1=\nu_2=0$. (a) displays $|A|^2$ vs x and (b) is the parametric plot of A vs x.

cally observe one-dimensional localized structures which are identified as the transverse structure of a finger (Fig. 4). As soon as a constant electric field is applied, this transverse structure drifts. Now the effect of the electric field can be investigated through a classical perturbation analysis. Let us look for a solution of Eq. (3) of the form

$$A(x,t)=A_0(x+X(T))+O(E_z^1)\ ,$$

where x is perpendicular to the finger axis, $A_0(x)$ is the isolated finger solution of the unperturbated equation ($E_z=0$), and $X(t)$ is slowly varying in time. Then, an easy but tedious computation shows that the previous development is a solution of Eq. (3) up to order 1, provided that

$$\frac{\partial X}{\partial t}=\kappa\cos(\omega t)+O(E_z^1)\ ,$$

where κ is a constant that depends on ν_0, ν_1, and on the chirality sign. This equation describes the oscillation of the finger perpendicularly to its axis, with an amplitude proportional to κ/ω. Therefore, high electric frequencies lead to stationary isolated fingers, while a dc electric field leads to a constant drift.

Now some remarks are in order. First, besides this perpendicular drift, experimental observations report a displacement of the finger along its axis. This effect, which has been called reptation [18], cannot be investigated in one space dimension; however, our two-dimensional numerical simulations show such an effect. Second, not all the rotating spirals observed in liquid crystal may be modeled by our equation. In particular, the spirals observed in Refs. [19] and [20], involving high birefringent optical patterns, are not covered by our analysis. In that case the deviation of the director from the homeotropic case is so large that our assumption (A is small) is no longer valid.

In conclusion, we have been able, using symmetry arguments, to write a Landau–de Gennes model of the unwinding transition of a cholesteric liquid crystal, in quite good qualitative agreement with both the experimental and theoretical thermodynamic phase diagrams. Our model is bidimensional, dynamical, and, though less precise than the usual 3D free-energy computations, able to explain the formation of spirals with a single given handedness.

We are very grateful to P. Coullet and S. Rica for helpful discussions. Also we acknowledge the INRIA where the numerical simulations were performed. The Institut de Nonlinéaire de Nice is UMR CNRS 129.

[1] A. T. Winfree, *The Geometry of Biological Time* (Springer, Berlin, 1980).
[2] C. Vidal and A. Pacault, *Nonlinear Phenomena in Chemical Dynamics* (Springer-Verlag, Heidelberg, 1981).
[3] E. Bodenschatz *et al.*, Physica D **61**, 77 (1992).
[4] F. T. Arecchi, G. Giacomelli, P. L. Ramazza, and S. Residori, Phys. Rev. Lett. **67**, 3749 (1991).
[5] H. P. Hinov and E. Kukleva, Mol. Cryst. Liq. Cryst. **109**, 203 (1984).
[6] M. Brehm, H. Finkelmann, and H. Stegemeyer, Ber. Bunsenges Phys. Chem. **78**, 883 (1974).
[7] W. E. L. Haas and J. E. Adams, Appl. Phys. Lett. **25**, 263 (1974); **25**, 535 (1974).
[8] A. E. Stieb, J. Phys. (Paris) **41**, 961 (1980).
[9] M. J. Press and A. S. Arrott, J. Phys. (Paris) **37**, 387 (1976).
[10] L. M. Blinov, *Electro-optical and Magneto-optical Properties of Liquid Crystals* (Wiley, New York, 1983).
[11] F. Lequeux, P. Oswald, and J. Bechhoefer, Phys. Rev. A **40**, 3974 (1989).
[12] P. Ribière, S. Pirkl, and P. Oswald, Phys. Rev. A **44**, 8198 (1991).
[13] A. M. Lyapunov, *Problème Général de la Stabilité du Mouvement,* Annals of Mathematics Studies No. 17. (Princeton University Press, Princeton, NJ, 1947).
[14] F. C. Frank, Discuss. Faraday Soc. **25**, 19 (1958).
[15] J. M. Gilli, M. Morabito, and T. Frisch, J. Phys. (France) (to be published).
[16] P. Ribière and P. Oswald, J. Phys. (Paris) **51**, 1703 (1990).
[17] J. M. Gilli and L. Gil, Liq. Cryst. (to be published).
[18] P. Ribière, Thèse d'Etat, Université de Lyon I, France (1992).
[19] J. M. Gilli and M. Kamayé, Liquid Crystals **11**, 791 (1992).
[20] M. Mitov and P. Sixou, J. Phys. II France **2**, 1659 (1992).